



**HAL**  
open science

## Reliable GNSS Positioning in Mixed LOS/NLOS Environments Using a 3D Model

Khairol Amali Bin Ahmad, Mohamed Sahmoudi, Christophe Macabiau, Aude Bourdeau, Grégory Moura

► **To cite this version:**

Khairol Amali Bin Ahmad, Mohamed Sahmoudi, Christophe Macabiau, Aude Bourdeau, Grégory Moura. Reliable GNSS Positioning in Mixed LOS/NLOS Environments Using a 3D Model. ENC 2013, European Navigation Conference, Apr 2013, Vienne, Austria. pp xxxx. hal-00943395

**HAL Id: hal-00943395**

**<https://enac.hal.science/hal-00943395v1>**

Submitted on 7 Feb 2014

**HAL** is a multi-disciplinary open access archive for the deposit and dissemination of scientific research documents, whether they are published or not. The documents may come from teaching and research institutions in France or abroad, or from public or private research centers.

L'archive ouverte pluridisciplinaire **HAL**, est destinée au dépôt et à la diffusion de documents scientifiques de niveau recherche, publiés ou non, émanant des établissements d'enseignement et de recherche français ou étrangers, des laboratoires publics ou privés.

# Reliable GNSS Positioning in Mixed LOS/NLOS Environments Using a 3D Model

Khairol Amali Bin Ahmad<sup>1</sup>, Mohamed Sahmoudi<sup>1</sup>, Christophe Macabiau<sup>2</sup>, Aude Bourdeau<sup>1</sup> and Grégory Moura<sup>3</sup>

<sup>1</sup>Institut Supérieur de l'Aéronautique et de l'Espace (ISAE), Toulouse, France

mail: Khairol-amali.AHMAD@etu.isae.fr, mohamed.sahmoudi@isae.fr

<sup>2</sup>École Nationale de l'Aviation Civile (ENAC), University of Toulouse

<sup>3</sup>OKTAL-SE, VIGOULET-AUZIL, France

**Abstract** – Reliable GNSS positioning is a very challenging task in harsh urban environment. The main source of error is due to non-line-of-sight (NLOS) reception and multipath phenomena. The effect of assuming a direct path in a NLOS propagation environment leads to serious degradation in accuracy. Instead of discarding all measurements which are found to be in NLOS conditions, we propose to properly use these observations to improve the positioning accuracy and integrity in harsh environments.

In this paper, we combine the sigma- $\epsilon$  variance model with a mean jump (i.e. NLOS bias) to model the pseudorange (PR) errors. First, we use a 3D model of the environment to detect the NLOS state of reception and to predict the NLOS bias related to the excess delay phenomenon. For reliable positioning, we use a C/No-based variance adjustment for the LOS PRs, and we subtract the bias from the NLOS PRs during the trilateration step of position computation. The performance of the proposed scheme is assessed using real data and compared to a standard Kalman filter without predicted information from the 3D simulator.

## BIOGRAPHIES

**Khairol Amali bin Ahmad** obtained a BSc in Electrical Engineering in 1992 from the United States Military Academy, West Point and an MSc in Military Electronic Systems Engineering in 1999 from Cranfield University. Since 2011, he is a PhD student at the French Institute of Aeronautics and Space (ISAE) working on reliability monitoring aspects of GNSS aided navigation systems for land vehicle applications in harsh environment.

**Mohamed Sahmoudi** received a PhD in signal processing and communications from Paris Sud University and Telecom Paris in 2004, and an M. S. degree in statistics from Pierre and Marie Curie University in 2000. During his PhD, he was an assistant lecturer at Ecole Polytechnique, then a lecturer at Paris Dauphine University. From 2005 to 2007, he was a postdoc researcher on GPS signal processing at Villanova University, PA, USA. In August 2007, he joined the ETS School of Engineering at Montreal, Canada, to work on GNSS RTK for precise

positioning. In December 2009, he became an associate professor at the French Institute of Aeronautics and Space (ISAE), Toulouse, France. His research interest includes weak multi-GNSS signals processing, multipath mitigation and multi-sensor fusion.

**Aude Bourdeau** received an engineer degree in mathematics and numerical modeling from INSA Toulouse in 2010. Since October 2010, she is preparing PhD at the French Institute of Aeronautics and Space (ISAE). Her research interest includes signal processing, GNSS navigation in challenging environment and GNSS signal tracking.

**Christophe Macabiau** graduated as an electronics engineer in 1992 from the ENAC in Toulouse, France. Since 1994, he has been working on the application of satellite navigation techniques to civil aviation. He received his PhD in 1997 and has been in charge of the signal processing lab of ENAC from 2000 to 2012. He is currently the head of the TELECOM lab of ENAC.

**Grégory Moura** graduated from the French Institute of Aeronautics and Space (ISAE-SUPAERO, Toulouse, France) in 2004. Since 2005, he has been working as a software engineer in the field of GNSS propagation simulation. He is currently SE-NAV product manager at OKTAL Synthetic Environment.

## I. INTRODUCTION

Reliable navigation entails quality of service in terms of accuracy, continuity, availability and also integrity especially for safety and liability critical applications. Even for the majority of comfort applications, while few meters of accuracy is sufficient, the positioning quality cannot be guaranteed in general when traversing a deep urban environment. The reason is that GNSS signal reception in harsh urban settings is notoriously challenging. Buildings and other objects surrounding the receiving antenna may block the direct line-of-sight (LOS) to many satellites, hence reducing the visibility. Often, the remaining signals have poor geometry and therefore degrade the position accuracy.

Apart from being blocked, the signals are also reflected and diffracted from the buildings and other objects. These signals distort measurements and bias the calculated position. If the signal is received only through reflections, the situation is known as non-line-

of-sight (NLOS) reception. Multipath interference is a phenomenon when the signal is received through multiple paths. Even though both the NLOS reception and multipath interference are often grouped together as 'multipath', they are actually separate phenomena that cause very different ranging errors. These degraded reception of multipath-contaminated LOS or NLOS are the dominant causes of reduced consumer grade positioning reliability in the urban environment. The effect of NLOS reception on a pseudorange (PR) measurement is associated to the additional path delay, i.e., the difference between the lengths of the path taken by the reflected signal as compared to the direct path, from satellite to the receiver. Hence, this error is always positive and, while typically tens of meters, is potentially unbounded [1]. Whenever high sensitivity receivers are used, the number of received NLOS signals can increase significantly due to the ability of the receivers to acquire much weaker signals.

Several existing techniques of multipath and NLOS mitigation may be categorized as hardware-based, signal processing in receiver and measurements domain [2, 3]. The work in [3] elaborates those techniques which make use of dual-polarization antenna, sky-pointing camera, beam forming antenna arrays, ground planes and choke rings. Their main limitations are usually related to cost, size, weights and power consumption. The common approaches to deal with the multipath problem through receiver-based techniques, such as the narrow correlators, do not bring the best improvement in the case of NLOS situations due to the absent of LOS signal. In post-receiver techniques (i.e., prior to the position calculation), one way to solve the NLOS situation problem is to identify and exclude the associated measurements in the navigation algorithm, by using techniques such as consistency-checking which is similar in concept with RAIM. However, this approach is not well adapted to positioning in harsh environments, when only degraded measurements may be available.

Under the poor conditions of satellites visibility, the positioning algorithms have to take into account the fact that the received signal may reach the antenna from a non-direct path with an additional distance. For this purpose, few works exist in the literature on constructive use of NLOS signals [4]. One option is to approximate the PR errors model of NLOS measurements so that the PR may still be usable for positioning. The bias can be treated either as a random variable, if a statistical characterization is available or as a deterministic quantity if it is somehow known or predictable.

Mixing the bias with the additive noise, the resulting term is considered as random error and may be modeled by a Gaussian mixture [5] since the NLOS measurements noise has been observed to be non-Gaussian, or by adapting the measurements variance [6]. In addition, authors in [7] shows that the measurement errors distributions depend on the observation window size. Over a short observation

period, PR errors can be modeled by a Gaussian distribution, with time-varying mean and variance.

In order to adopt such measurements error-model based processing, a reliable decision on the reception state of the received signal (i.e. LOS or NLOS status) is needed. In [5], authors use the Jump Markov System as probabilistic model with received signal-to-noise-ratio (SNR) as indicator of the LOS/NLOS reception state. However, although it has the potential to be used independently of any heavy environment assumptions, SNR estimation is a critical issue in harsh environments, thus the decision based on contaminated information will affect the result. Furthermore, SNR values which are obtained from PRs collected in one area will not be representative any more for another area since the transition between LOS and NLOS depends greatly on the geometrical structure of the location.

In this paper, we analyze the benefit brought in the comfortable situation where a 3D city model can be used to predict the reception state and the bias of each satellite as a potential alternative. We integrate tightly these simulated information in the Kalman filter computing the PVT (position, velocity, time) and we assess the performance of the proposed approach.

## II. PREDICTING LOS/NLOS CONDITION VIA 3D MODEL

As 3D city models becoming more accurate and widely available, there are growing interests in their application to predict satellite reception availability. The works of [8, 9] used 3D city model to predict GNSS availability considering LOS, diffracted and re-radiated signals. In [10], the authors used 3D digital map in order to detect and mitigate multipath in real-time where a ray tracing algorithm is used to check if satellite signals are reflected or blocked. The suspicious PRs are simply excluded from the observation set. 3D model along with camera image were used in [11] to filter out the PR measurements which are considered to be NLOS based on the comparison of the actual satellite elevation angle with the critical elevation angle calculated using the 3D model. In [12] the authors use a 3D model to predict the geometric paths of NLOS signals so that they may be used constructively in order to obtain enough information to compute the user's position in harsh urban environment.

In this work, we use SE-NAV software [13] to predict the signal reception of GNSS systems such as GPS into 3D virtual scenes of known urban areas. The propagation of signals is based on a ray-tracing algorithm that computes the shadowing and multipath effects. SE-NAV uses geometric optics to calculate the reflected, diffracted and transmitted rays. Based on these multiple rays that reach the receiver, the LOS or NLOS reception state of a satellite is provided. The position of the satellites and the receiver must be known. The satellite positions are calculated based on the ephemeris data whereas the positions along the trajectory are obtained from the receiver.

A. SE-NAV – Deterministic simulator of GNSS reception in constrained environment

SE-NAV simulates the propagation of GNSS signals in constrained environment (urban area, indoor etc.). This software, developed by the company OKTAL Synthetic Environment, embeds a GPU Raytracing kernel to compute the masks and the multipath (reflections, transmission and diffractions) generated by the objects/buildings near the receiver.

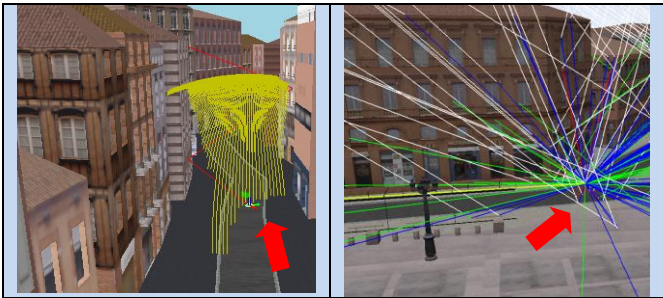


Figure 1: Left: Mask sphere showing the masking impact. Right: Example of multipaths reception in an urban area. – 3D Red arrows point to the location of the receiver

1) Raytracing and BVH optimization

A Raytracing algorithm consists in finding the intersections between a ray and a defined geometry as fast as possible. SE-NAV uses geometries made of a large number of triangles. For high frequency asymptotic EM simulation, a large number of such intersections has to be computed. A very naïve approach would require  $N \cdot M$  ray-triangle intersections,  $N$  being the number of triangles and  $M$  the number of rays. Except for very simple situations, this cost is prohibitive, hence the need for acceleration methods. Among these methods, the Bounding Volume Hierarchy (BVH), an object-based subdivision structure is chosen. The principle is to build a tree-structure of a set of triangles. Each triangle is stored in a leaf of the tree. Each internal node stores for each of its children the bounding volume of the descendant triangles. A bounding-volume hierarchy is built according to the location of each triangle of the database, trying to minimize the extent and the number of nodes.

Once the structure is built, the intersection between a ray and the scene is done by traversing the tree recursively from the root. A child is processed only if the ray intersects its bounding volume. If the two children are traversed, the process is repeated first on the children closest to the ray origin. If the child is a leaf, the ray is intersected with all triangles contained in the leaf, potentially updating the intersection data. Traversal is stopped as soon as no intersection closer than the current one can be found. This method decreases drastically the ray-scene intersection computation time, computing only  $O(\log(N) \cdot M)$  intersections instead of  $N \cdot M$  for  $N$  triangles and  $M$  rays.

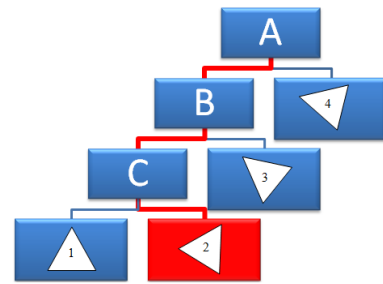
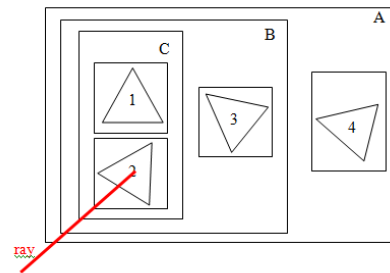


Figure 2: Top: Triangles sorting – Bottom: Bounding-volumes hierarchy

2) GPU Resources

The Raytracing kernel has been developed in CUDA 4.0 language and uses the GPU resources in order to compute masks and multipath in record times (1000 times quicker in optimal configurations). SE-NAV uses GPU to find rays and CPU to filtrate them according to Geometrical Optics rules.

SE-NAV runs on NVIDIA Graphics board series 8 or later. The video memory shall be greater than 512 Mo and the compute capability rate greater than 1.1 (atomic operations shall be allowed)

3) Model Outputs

SE-NAV uses Geometrical Optics to model reflections and transmissions and Uniform Theory of Diffraction to detect signal's diffractions on the edges of the objects. As SE-NAV uses a deterministic method, the software can calculate and display the geometry of each ray reaching the receiver and then computes the total link budget and errors needed to forecast the local pseudorange. Thanks to the different DOPs provided as an output and also the visibilities of the constellation (LOS, NLOS, and hidden satellite), the user can assess the availability of the navigation system and its performance within a given area.

SE-NAV computes a link budget and provides in output the received power per multipath and per channel. To do so, SE-NAV assesses the main source of attenuations during the propagation of the signal in the environment.

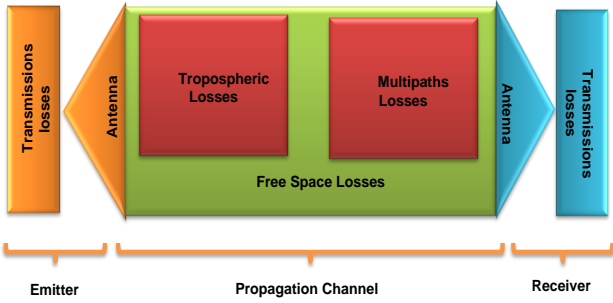


Figure 3: Link budget

SE-NAV takes into account cabling losses, antenna gain (satellite and receiver), free space losses, tropospheric losses and multipath losses. SE-NAV computes the complete field (modulus and phase) and therefore models interferences and fading effects. SE-NAV also provides Signal-To-Noise Ratio and composite power (i.e. integrated power for a given channel).

### B. Reliability of 3D model for reception state prediction and NLOS bias prediction.

The reliability of the computed position depends on the reliability of the PR measurements model. In this work, distribution of the errors on the final navigation solution depends on the quality of the decision taken on the NLOS and LOS situation as obtained from the 3D model. Hence, it is crucial to determine the quality of the SE-NAV LOS/NLOS identification as well as the impact of this decision on the error modeling.

While there have been several works such as in [8, 9] where prediction of satellite availability based on 3D model were studied, there has not been many works studying the LOS/NLOS state of reception based on 3D model. One of the approaches in categorising the LOS/NLOS state of reception is to base on the received C/No [5]. In this work, we compare the conformity of state reception prediction provided by the 3D model with that one obtained using the C/No value. An example of conformity is when SE-NAV predicts a received signal as a NLOS and the C/No of that signal is below the set threshold (a value between 40 and 30 dB-Hz).

Apart from predicting the reception state, the 3D model is also utilized to predict the NLOS bias statistic, which is to be used for the PR corrections. In this case, how close the predicted bias to the measured NLOS bias will affect the similarity of the final computed position.

## III. POSITIONING APPROACH WITH NLOS SIGNALS

### A. LOS/NLOS Pseudoranges measurements model

Over a relatively long observation window, the NLOS measurements error has been observed to have a non-Gaussian distribution and may be approximated by a Gaussian mixture [5], as illustrated in Figure 4.

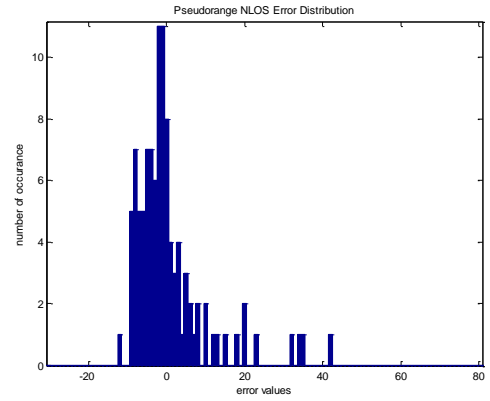


Figure 4: NLOS error distribution

However, for a short observation window, the most common approach consist of modeling the pseudorange error as Gaussian distribution with a time-varying mean and variance [7] as illustrated in Figure 5. Here, the error distributions of the same satellite are shown within different 40 seconds windows where it can be seen their change in the mean and variance.

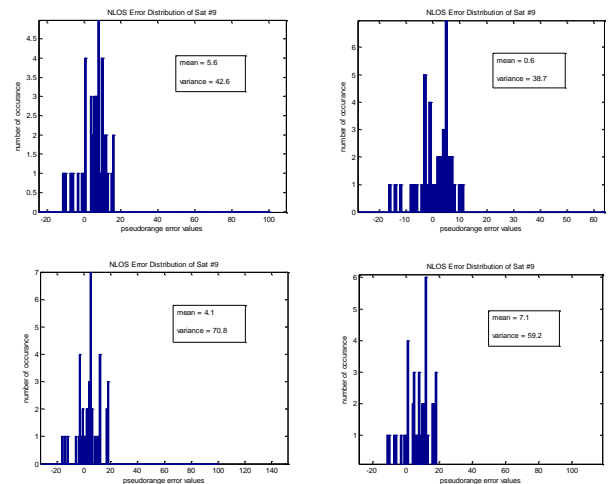


Figure 5: PR error distributions in short observations periods.

In the NLOS case, the presence of only reflected signals introduce a jump on the mean value as a result of the extra distance. In the case of degraded LOS path, an additional variance is introduced as increase of the uncertainty on the direct path. Accordingly, we model separately these effects of the degraded LOS noise and NLOS bias on the PR measurements error.

For the case of multipath degraded LOS reception, implementing the signal-to-noise ratio based variance model, i.e. the SIGMA- $\epsilon$  model, would improve the positioning accuracy in the urban environment [6, 14]. The covariance matrix of the observation can be constructed as  $\mathbf{R} = \text{diag}(\sigma_1^2, \sigma_2^2, \dots, \sigma_k^2)$  where

$$\sigma_k^2 = a + b \cdot 10^{\frac{-C/N_0}{10}} \quad (1)$$

and  $\sigma_k^2$  is the variance of the  $k^{\text{th}}$  observation. The constant  $a$  and  $b$  are determined depending on the environment and user equipment.

The PR measurement model is commonly expressed as the true distance  $d$  between the receiver and satellite, plus with several other types of errors. For each satellite at  $k^{\text{th}}$  point in time, the pseudorange  $\rho$  can be written as,

$$\rho_k = d_k + c \cdot dt_k^{\text{sat}} + c \cdot dt_k^{\text{rcv}} + \text{atmo}_k + m_k + \epsilon_k \quad (2)$$

with  $c \cdot dt$  represents clock offset (satellite or receiver),  $\text{atmo}$  represents both the ionospheric and tropospheric delays.  $m$  is the multipath delay and  $\epsilon$  is the receiver noise. In harsh urban environment,  $m$  is the major contributor of error and could consist of the mixed LOS/NLOS conditions. Once the ionospheric, tropospheric, ephemeris and clock errors are compensated, the model is reduced to the following expression,

$$\rho_k = d_k + m_k + \epsilon_k \quad (3)$$

To further illustrate the LOS/NLOS conditions in the multipath, we may rewrite the equation as [15]

$$\rho_k = d_k + m_k + b_k w_k \quad (4)$$

$$\text{where: } m_k = \begin{cases} 0, & \text{if LOS condition} \\ m_{\text{NLOS}}, & \text{if NLOS condition} \end{cases}$$

$$b_k = \begin{cases} \sigma, & \text{if LOS condition} \\ \sqrt{\sigma^2 + \sigma_{\text{NLOS}}^2}, & \text{if NLOS condition} \end{cases}$$

and  $w_k$  is the centralized zero mean white Gaussian noise  $\mathcal{N}(0,1)$ . Then, in the case of NLOS, the affected measurement becomes

$$\rho'_k = \rho_k - m_{\text{NLOS}} = d_k + b_k w_k, \quad (5)$$

$$\text{and } b_k = \sqrt{\sigma^2 + \sigma_{\text{NLOS}}^2}$$

## B. Integration of the 3D-based Bias Estimation in the PVT Kalman Filter

In this paper, the well-established Extended Kalman Filter (EKF) is chosen as the positioning estimator for post-processing the measured PRs. Based on the measurement model in (4), the state equation can be provided by:

$$\mathbf{X}_{k+1} = \mathbf{F}\mathbf{X}_k + \mathbf{v}_k \quad (6)$$

where  $\mathbf{X}$  is the state vector,  $\mathbf{F}$  is the state transition matrix and  $\mathbf{v}$  is the process noise with zero mean Gaussian distribution.

$$\mathbf{X}_k = [p_k, \dot{p}_k, ct_k, \dot{ct}_k]^T \quad (7)$$

where  $p_k$  is the  $x_k, y_k, z_k$  position coordinates,  $\dot{p}_k$  are the velocities,  $ct$  is the clock bias and  $\dot{ct}$  is the clock drift.

$$\mathbf{F} = \begin{bmatrix} \mathbf{I} & T_s \mathbf{I} & 0 & 0 \\ 0 & \mathbf{I} & 0 & 0 \\ 0 & 0 & 1 & T_s \\ 0 & 0 & 0 & 1 \end{bmatrix} \quad (8)$$

where  $\mathbf{I}$  is the identity matrix and  $T_s$  is the sampling period.

$$\mathbf{v}_k \sim \mathcal{N}(0, \text{diag}(\mathbf{Q}_1, \mathbf{Q}_2)) \quad (9)$$

where

$$\mathbf{Q}_1 = \begin{bmatrix} \frac{T_s^3}{3} \sigma_a^2 \mathbf{I} & \frac{T_s^2}{2} \sigma_a^2 \mathbf{I} \\ \frac{T_s^2}{2} \sigma_a^2 \mathbf{I} & T_s \mathbf{I} \end{bmatrix} \quad (10)$$

and

$$\mathbf{Q}_2 = \begin{bmatrix} \sigma_b^2 T_s + \frac{T_s^3}{3} \sigma_d^2 & \frac{T_s^2}{2} \sigma_d^2 \\ \frac{T_s^2}{2} \sigma_d^2 & T_s \sigma_d^2 \end{bmatrix} \quad (11)$$

The clock bias variance  $\sigma_b^2$  and clock drift variance  $\sigma_d^2$  depend on the quality of the receiver, while the acceleration variance  $\sigma_a^2$  depend the motion of the receiver.

Based on the prediction from the 3D model of the LOS/NLOS reception condition of each satellite, the PR measurement and its variance are treated accordingly. If the measured PR is predicted as a LOS signal, its covariance is adapted to the value using equation (1). However, if the measurement is predicted as a NLOS reception, the NLOS bias  $m_{\text{NLOS}}$  is predicted from SE-NAV and subtracted from PR measurement and the NLOS variance  $\sigma_{\text{NLOS}}^2$  is included in the covariance as described by equations (4) and (5).

The observation equation can be formulated as,

$$\mathbf{z}_k = \mathbf{h}(\mathbf{X}_k) + \mathbf{m}_k + \mathbf{b}_k \mathbf{w}_k \quad (12)$$

where  $\mathbf{h}$  describes the non-linear dependence of the observations on the state. The observation covariance is,

$$\mathbf{b}_k \mathbf{w}_k \sim \mathcal{N}(0, \mathbf{R}) \quad (13)$$

where  $\mathbf{R}$  depends on the LOS/NLOS condition of the reception state.

Usually, the values for the bias and variances of NLOS errors are obtained based on the PR error distributions. In this study, the PR error values are initially calculated based on the difference between the measured PRs vis-à-vis the reference PRs which are acquired by computing the distance from the satellite positions and the reference positions. However, such approach would be limited for positioning applications with a fixed and predetermined route.

In an attempt to make the application to be less restrictive, this work further considers the PR errors values generated from the predictions of the 3D-model. The delays of the PR ray-tracings from the 3D-model are treated as the errors of the PR measurements.

## C. Data Collection, Equipment and Software

In this work, the measurements were obtained from a trajectory around Toulouse, France (Figure 6). The area represents a deep urban environment with narrow streets and buildings alongside the streets.

The GPS receiver used for the PR measurements is the u-blox LEA-4T receiver while the NovAtel SPAN system is used for the reference trajectory. The measurement was sampled at 1 Hz. All data processing was accomplished using Matlab and SE-NAV





Figure 6: Reference trajectory in Toulouse, France.

#### IV. RESULTS

##### A. Estimation of Variance (C/No) Model Parameters

In order to implement the SIGMA- $\varepsilon$  variance model as in equation (1), the values for parameters  $a$  and  $b$  have to be determined. This is achieved by fitting the

$Standard\ Deviation = \sigma_k = \sqrt{a + b \cdot 10^{\frac{-C/No}{10}}}$  to the plot of absolute pseudorange errors vs. C/No. The standard deviation is simply the square root of the variance in equation (1) and the absolute pseudorange errors are the magnitude of the pseudorange errors. Figure 7 shows an example of the plot and Table 1 lists all the determined  $a$  and  $b$  values per visible satellite during data collection.

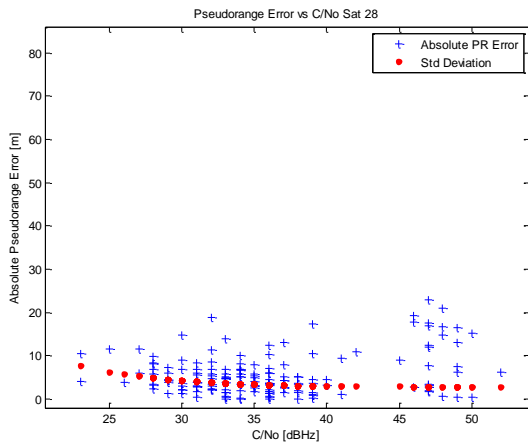


Figure 7: C/No variance model.

It is noted that during this early stage of research, the number of sampled measurements is rather small. Nevertheless, they are sufficient at the moment.

##### B. LOS/NLOS Prediction by SE-NAV

Determination between LOS/NLOS reception is indeed a challenging task. Here, the LOS/NLOS prediction by SE-NAV is compared to the received C/No values of the PR measurements. Threshold

values of 40, 38 and 30 dB-Hz are used for comparisons. Percentages of conformity between SE-NAV prediction and C/No values are listed in Table 2.

Table 1: List of parameters for variance (C/No) model obtained by curve fitting with the absolute PR errors

Sat	$a$	$b$
5	164	$-1 \times 10^4$
8	115	$1 \times 10^4$
9	127	3336
10	171	$2 \times 10^4$
15	136	$-1 \times 10^4$
17	325	1339
18	48	$2 \times 10^4$
24	982	-4649
26	55	$-1 \times 10^4$
27	29	-7603
28	8	$1 \times 10^4$

Table 2: Conformity between SE-NAV LOS/NLOS prediction and the C/No values

Sat	C/No = 40 dB-Hz	C/No = 38 dB-Hz	C/No = 30 dB-Hz
5	61 %	45 %	2 %
8	98 %	95 %	48 %
9	89 %	87 %	54 %
10	86 %	82 %	75 %
15	64 %	47 %	5 %
17	100 %	100 %	62 %
18	100 %	100 %	72 %
24	100 %	100 %	100 %
26	91 %	80 %	14 %
27	94 %	93 %	38 %
28	93 %	83 %	15 %
Total	89 %	83 %	44 %

These C/No values may also be cross referenced with the elevation angle of the satellites since the signals of the lower elevation satellites are more likely to be received as NLOS in the urban environment as compared to those of the higher elevation ones. In Figure 8, satellites with lower than  $26^\circ$  elevation tend to be the satellites with higher conformity with the SE-NAV LOS/NLOS prediction.

##### C. Results on Position Estimation

As a base of comparison, the error sequence of position estimation with NLOS bias correction is plotted against the error sequence of position estimation using the variance (C/No) only (i.e., without considering LOS/NLOS reception). Figure 9 (a) shows the comparison in 3D while Figure 9 (b) and 9 (c) are their respective error plots in ENU format.

From Figure 9 (a), it can be seen that the estimation with NLOS bias correction was generally better than the performance of the position estimation using only the variance (C/No) model. After about the 100<sup>th</sup> sample it can be said that both estimators

seemed to converge on more or less of equal performance at the end.

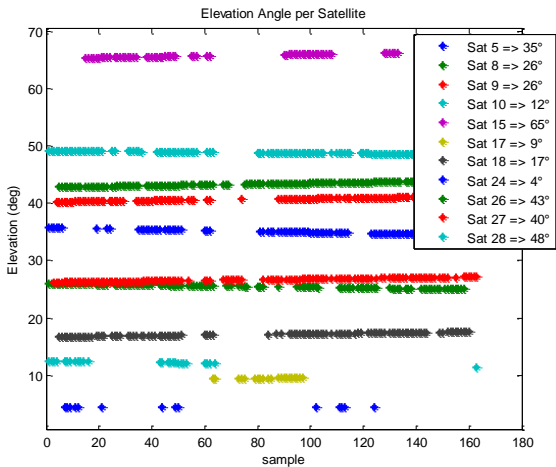


Figure 8: Elevation angle per satellite

When comparing their performance in the ENU format, it is obvious that both of the error patterns of the two position estimation approaches are strongly influenced by their error estimation in the height direction. If the height error is discounted, their performance can be compared in the XY plane (Figure 10) where their performances are much better. The estimation with bias correction was able to reduce several large error values that exist in the estimation with variance (C/No) around the 37<sup>th</sup>, 66<sup>th</sup> and 87<sup>th</sup> samples.

#### D. Bias Prediction by SE-NAV

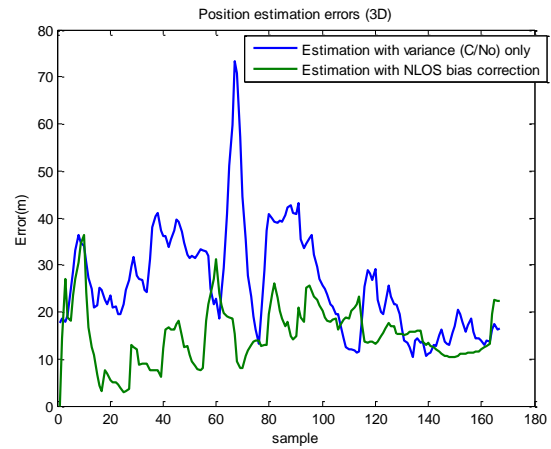
Apart from predicting the LOS/NLOS reception, this study also attempts to use the 3D model to predict the NLOS bias. Figure 11 shows the comparison of the measured bias versus the predicted bias for Sat 5. While there is some similarity in the patterns, the values of the bias are quite different between them. Further research could be pursued in order to improve NLOS bias prediction by the 3D model.

Figure 12 is the position error comparison between the positions estimate using measured bias for PR correction against the positions estimate using bias predicted by SE-NAV for the PR correction. The plot is in the XY plane to discount the effect of the estimation error in the height direction. Despite the difference between their bias values as indicated in Figure 11 before, their positioning performances in XY plane are quite similar in general.

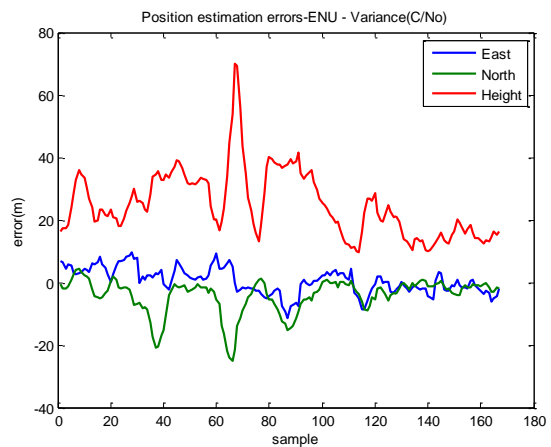
## V. CONCLUSIONS

This paper proposed the utilization of 3D model in predicting the LOS/NLOS reception state. In addition, the 3D model is also used to predict the NLOS bias of the measurements. These simulated information is used for correction of the PR error according to the LOS or NLOS case and then processed in the PVT computation algorithm. The ability of the 3D model to

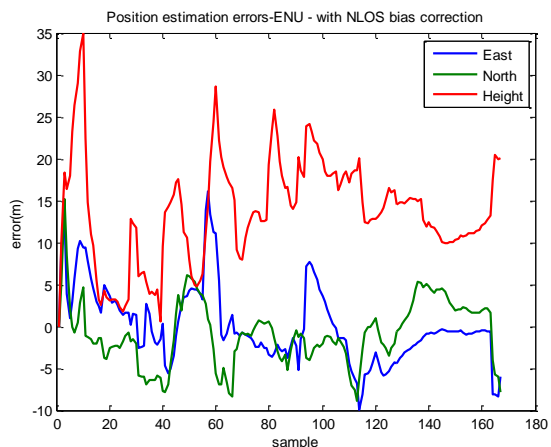
predict LOS/NLOS was found to be encouraging when compared with other indicators such as C/No and satellite angle of elevation.



(a)



(b)



(c)

Figure 9: (a) Error of position estimates in 3D, (b) and (c) Error estimates in East, North and Height.

The ability of the 3D model to predict the NLOS bias was deemed modest and not concluding for the short processed data. Further research and analysis are required to validate the quality of the predictions by



3D model. In term of the bias prediction, other technics of exploiting better the 3D information may be developed.

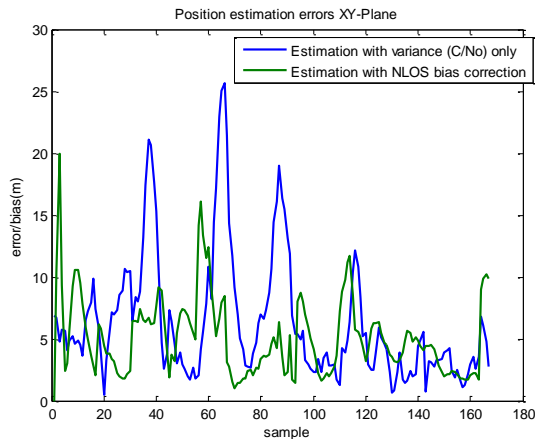


Figure 10: Error of position estimates in XY plane

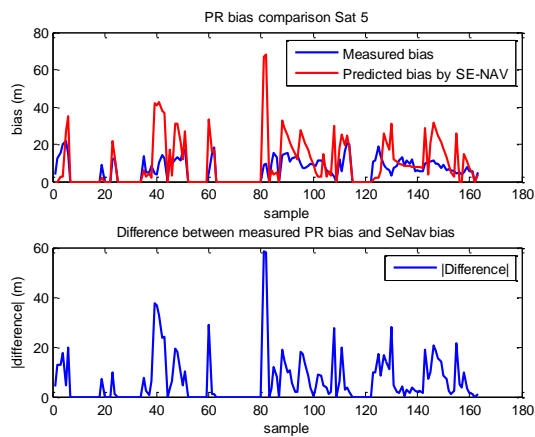


Figure 11: Error of position estimates in XY plane

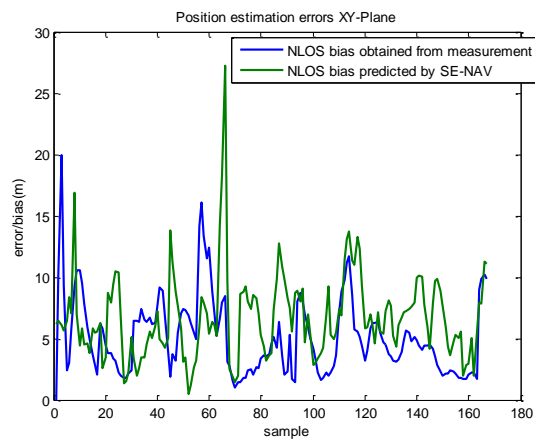


Figure 12: Measured NLOS bias against SE-NAV predicted NLOS bias by

#### ACKNOWLEDGMENT

The authors would like to thank Benoit Priot for providing some assistance for the experimental work.

#### REFERENCES

- [1] J. Cosmen-Schortmann, M. Azaola-Saenz, M. A. Martinez-Olague, M. Toledo-Lopez, 'Integrity in urban and road environments and its use in liability critical applications', Position, Location and Navigation Symposium, 2008 IEEE/ION, 5-8 May 2008.
- [2] M. Sahnoudi and R. J. Landry, 'Multipath mitigation techniques using maximum-likelihood principle', Inside GNSS, November/December 2008, pp.24–29.
- [3] P. D. Groves, Z. Jiang, L. Wang, and M. K. Ziebart, 'Intelligent Urban Positioning using Multi-Constellation GNSS with 3D Mapping and NLOS Signal Detection', Proc. of the 25th International Technical Meeting ION GNSS'12, Nashville, September 2012, pp. 458-472.
- [4] W. Ke, and L. Wu, 'Mobile Location with NLOS Identification and Mitigation Based on Modified Kalman Filtering', Sensors. 2011, 11(2), pp.1641-1656.
- [5] N. Viandier, D.F. Nahimana, J. Marais and E. Duflos, 'GNSS Performance Enhancement in Urban Environment Based on Pseudo-range Error Model', Position, Location and Navigation Symposium, 2008 IEEE/ION, 5-8 May 2008.
- [6] A. Wieser, M. Gaggl, and H. Hartinger, 'Improved positioning accuracy with high sensitivity GNSS receivers and SNR aided integrity monitoring of pseudo-range observation', in Proc. of the 18<sup>th</sup> International Technical Meeting ION GNSS'05, pp. 1545–1554, 2005.
- [7] M. Spangenberg, J.Y. Tourneret, V. Calmettes, O. Julien and G. Duchateau, 'Detection of Variance Changes and Mean Value Jumps in Measurement Noise for Multipath Mitigation in Urban Navigation', Journal of The Institute of Navigation, vol. 57(1).
- [8] L. Wang, P. D. Groves, and M. K. Ziebart, 'Multi-Constellation GNSS Performance Evaluation for Urban Canyons Using Large Virtual Reality City Models', Journal of Navigation, Vol. 65, No. 3, 2012, pp. 459-476
- [9] J. Bradbury, 'Prediction of Urban GNSS Availability and Signal Degradation Using Virtual Reality City Models', Proc. of ION GNSS'07, Fort Worth, TX, September 2007.
- [10] M. Obst, S. Bauer, and G. Wanielik, 'Urban multipath detection and mitigation with dynamic 3D maps for reliable land vehicle localization', in Proc. of the IEEE/ION PLANS'12, Myrtle Beach, SC, April 2012.
- [11] F. Peyret, D. Bétaille, and F. Mougél, 'Non-Line-Of-Sight GNSS signal detection using an on-board 3D model of buildings', 11th International Conference on ITS Telecommunications (ITST), pp.280,286, 23-25 Aug. 2011.
- [12] A. Bourdeau, M. Sahnoudi, and J.Y. Tourneret, 'Tight Integration of GNSS and a 3D City Model for Robust Positioning in Urban Canyons', in Proceedings of the ION conference GNSS 2012, Nashville, TN, USA, Sept 2012.
- [13] OKTAL-SE web site <http://www.oktal-se.fr/>
- [14] H. Kuusniemi, 'PhD Thesis: User-Level Reliability and Quality Monitoring in Satellite-Based Personal Navigation', Tampere University of Technology, 2005.
- [15] J. F. Liao, B. S. Chen, 'Robust Mobile Location Estimator with NLOS Mitigation using Interacting Multiple Model Algorithm', IEEE Trans. on Wireless Com., 5(11), Nov 2006.
- [16] A. Bourdeau, M. Sahnoudi, and J.Y. Tourneret, 'Prediction of NLOS GNSS Signals with a 3D Model of the User Urban Environment', in Proceedings of the ENC'13, conference, Vienna, April 2013.